JGR Space Physics

RESEARCH ARTICLE
10.1029/2019JA026799

Characteristics of the Occurrence of Ion Upflow in Association With Ion/Electron Heating in the Polar Ionosphere

Eun-Young Ji[1,2], Geonhwa Jee[1,3], and Changsup Lee[1]

[1]Korea Polar Research Institute, Incheon, South Korea, [2]Now at School of Space Research, Kyung Hee University, Yongin, South Korea, [3]Department of Polar Science, Korea University of Science and Technology, Daejeon, South Korea

Key Points:
- Ambipolar electric field with electron heating may be more effective to produce ion upflow when the ions are also simultaneously heated
- Diurnal variation of ion upflow occurrence shows a double peak structure during the day and a deep minimum at dusk
- Maximum occurrence appears in December solstice but minimum in June solstice

Correspondence to:
G. Jee,
ghjee@kopri.re.kr

Citation:
Ji, E.-Y., Jee, G., & Lee, C. (2019). Characteristics of the occurrence of ion upflow in association with ion/electron heating in the polar ionosphere. *Journal of Geophysical Research: Space Physics*, *124*, 6226–6236. https://doi.org/10.1029/2019JA026799

Received 5 APR 2019
Accepted 22 JUN 2019
Accepted article online 30 JUN 2019
Published online 22 JUL 2019

Abstract We investigate the statistical characteristics of the ion upflow occurrence in association with ion and electron heatings in the polar ionosphere using the European Incoherent Scatter Svalbard Radar during the period of 2000–2015. The ion upflow events are classified as four types: with ion temperature increase (Type 1), with electron temperature increase (Type 2), with both ion and electron temperature increases (Type 3), and without any temperature increase (Type 4). These four types of upflow events are statistically analyzed with various geophysical conditions. We found that the overall occurrence of ion upflow is highest for Type 3 and then followed by Type 2, Type 1, and Type 4. This result indicates that the ion upflow is highly associated with soft particle precipitation induced electron heating, which becomes more effective with simultaneous friction induced ion heating. The statistical characteristics of ion upflow is summarized as follows: (1) It is most highly distributed in the daytime with a double peak structure but a deep minimum at dusk, (2) the highest occurrence appears at about 350- to 450-km altitude for most of local time but extended to higher altitude near the magnetic local noon, (3) the ions mostly reach only up to about 200 km above their initiated altitudes, (4) it tends to increase with magnetic activity, particularly during the daytime, but (5) decreases and distributed at higher altitude with increasing solar activity, and (6) finally, the maximum occurrence appears in December solstice but the minimum in June solstice for most of local times.

1. Introduction

It is well known that ions can move upward along the geomagnetic field lines with velocity ranging from hundreds to thousands of meters per second in the polar ionosphere. The upward moving ions reaching the escape velocity of the Earth's gravity can flow into the magnetosphere, which is called the “ion outflow.” These outflowing ions can be a significant source of magnetospheric plasma. More frequently, however, the upward moving ions do not reach the escape velocity and fall back to the Earth's atmosphere. Although it is not yet fully understoodd how “ion upflow” becomes “ion outflow” with additional accelerating forces at high altitudes, it is important to understand the fundamental characteristics of the ion upflow whether it becomes ion outflow or not.

The main physical mechanisms causing the ion upflow are proposed as follows: (1) The solar extreme ultraviolet radiation and energetic particle precipitation ionize atmospheric constituents and produce secondary electrons with enough energy to move upward under the gravitational forces. The upward moving electrons pull up the ions with them via the ambipolar electric field existing between electrons and ions (e.g., Burchill et al., 2010; Liu et al., 1995; Moen et al., 2004; Ogawa et al., 2003; Zhao et al., 2016). (2) The ion-neutral frictional heating driven by plasma convection increases ion temperature. The increased ion temperature then creates the vertical pressure gradient to cause upward motion of the ions along the vertical magnetic field line in the polar *F* region ionosphere; in other words, it increases the scale height of ions to bring them to higher altitude (e.g., Keating et al., 1990; Loranc et al., 1991; Ma et al., 2018; McCrea et al., 2000; Winser et al., 1989; Zhang et al., 2016). (3) The third mechanism is the velocity shear-driven instability which produces transverse ion heating (Ganguli et al., 1994; Liu & Lu, 2004).

A number of studies have been conducted to investigate the statistical characteristics of the ion upflow in the polar ionosphere in relation to the first and second mechanisms. For instance, it was found that ion upflow observed with the European Incoherent Scatter (EISCAT) Svalbard radar occurs mostly in the dayside and

the maximum occurrence of ion upflow is seen at around the magnetic local noon (e.g., Buchert et al., 2004; David et al., 2018; Liu et al., 2001; Ogawa et al., 2003; Ogawa et al., 2009). One of the main drivers of the daytime ion upflow is known to be a soft particle precipitation in the cusp region. Soft particles (<500 eV) entering into the cusp region ionizes the neutral particles and produces heated electrons, which move upward together with ions via ambipolar electric field. Ogawa et al. (2003) reported that the soft particle precipitation is the dominant source mechanism causing the ion upflow in the dayside polar cap region, based on the observations from EISCAT Svalbard Radar (ESR) and DMSP satellite. Moen et al. (2004) showed a one-to-one relationship between poleward moving auroral forms and ion upflows in the cusp region, which indicates that the individual events of soft particle precipitation induce corresponding upflow events. Zhao et al. (2016), using FAST satellite data, also showed that the peak of the O^+ upflow occurrence at magnetic local time (MLT) noon is related to the soft particle precipitation in the cusp region.

On the other hand, Endo et al. (2000) suggested that heavy ions such as O^+ require other physical processes in addition to ambipolar electric field to accelerate upward in the polar ionosphere since the heavy ions driven by ambipolar electric field alone may not reach to the upwelling speed fast enough to overcome the Earth's gravity. Loranc et al. (1991) studied the vertical bulk ion drift data from the DE-2 satellite between 200- and 1,000-km altitudes. They found that the ion flows are predominantly upward near the cusp region and these upflowing ions are associated with high ion temperature caused by frictional heating. McCrea et al. (2000) reported the observation of ion upflow event with high ion temperature associated with ion-neutral frictional heating from the ESR observations. Zhang et al. (2016) reported the dynamics of oxygen ion upflow associated with a polar cap patch at the center of the polar cap region during a geomagnetic storm. They found strong fluxes of upwelling O^+ induced by frictional heating that is associated with rapid antisunward flow of the plasma patch. More recently, Ma et al. (2018) also found that the highest ion upflow occurrence in the polar cap appears with the highest convection speeds.

There have also been several studies indicating that the ion upflow is accompanied by both the elevated ion and electron temperatures in the cusp ionosphere. For example, Wu et al. (2000), using DE-2 satellite observations for the ionosphere, suggested that both the soft particle precipitation and frictional ion heating could be responsible for ion upflow and the former may be more effective during the daytime, while the latter may be more efficient during the nighttime. Liu et al. (2001) performed a statistical study of ion upflow using EISCAT and ESR observations, which suggested physical processes such as soft particle precipitation and $E \times B$-driven frictional heating responsible for the ion upflow in the F region heights depending on MLT and geomagnetic activity. Ogawa et al. (2009) also found that approximately 50 % of dayside ion upflows were accompanied by enhanced ion and electron temperatures at 400-km altitude. Skjæveland et al. (2011) observed the ion upflow events driven by frictional heating as well as the soft particle precipitation in the cusp region using the ESR observations.

These previous studies seem to indicate that there is yet no evident relationship between electron and ion heating to cause the ion upflow in the F region height near the polar cap region. The aim of this study is to better understand the relationship by investigating the height distributions of ion upflow occurrence as well as the MLT distributions associated with both electron and ion heatings from the 15-yearlong EISCAT Svalbard Radar (ESR) observations for different season and solar/geomagnetic condition.

2. Data and Analysis

We used the altitude profiles of ion velocity obtained from the EISCAT Svalbard Radar (ESR; 42 m) during the period between 2000 and 2015 to investigate the statistical characteristics of the ion upflow events. The ESR is located in Longyearbyen, Svalbard (78.1°N, 16.0°E), which is in the auroral and polar cap regions depending on local time and magnetic activity. The ESR 42-m dish antenna is fixed along the nearly vertical magnetic field line to monitor the ionospheric parameters along the local geomagnetic field lines such as electron density, ion and electron temperatures, and line-of-sight (i.e., field-aligned) velocity of the ions. We used the field-aligned ion velocity data with a 1-min time resolution for this analysis. The height resolution of each measurement of density profile varies with height. It is about 10–20 km at lower altitudes but increases to about 40 km at high altitudes (~500-km altitude). The ESR data were obtained from the EISCAT database at National Institute of Polar Research and the Madrigal database. The altitude range of data is restricted from 200- and 600-km altitudes because the incoherent scatter radar (ISR) observations

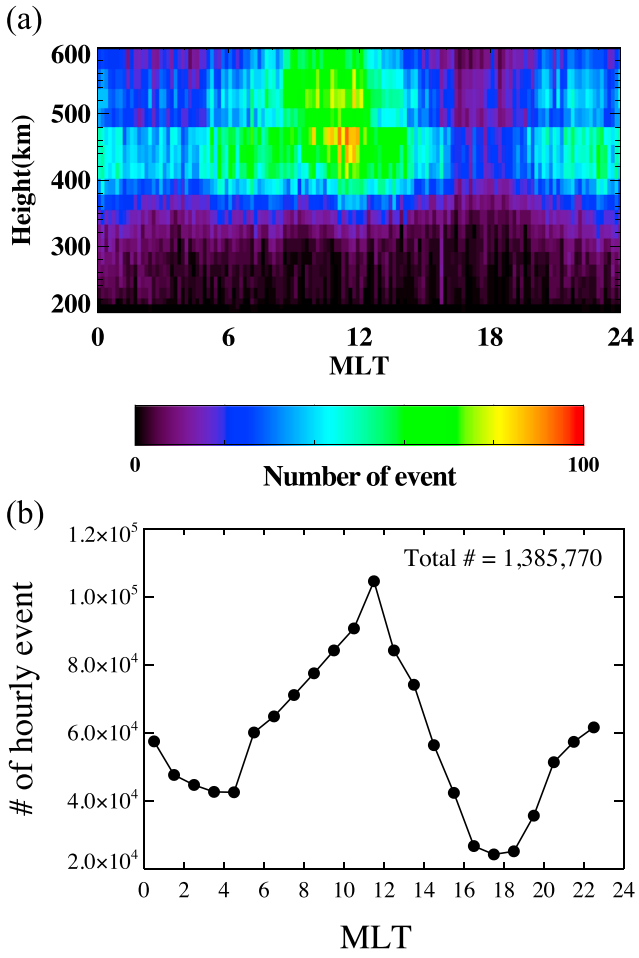

Figure 1. Height versus magnetic local time (MLT) distributions of the number of ion upflow events for the entire observation period (a) and diurnal variations of the height-integrated hourly number of events (b). The total number of events during the observation period is also given.

including ESR often suffer from low signal-to-noise ratio at high altitudes and the strong interactions with dense atmosphere at low altitudes (David et al., 2018).

The identification of ion upflow requires certain criteria for selecting ion upflow events (e.g., Foster et al., 1998; Keating et al., 1990; Liu et al., 2001; Ogawa et al., 2009, 2010). In this study, the ion upflow events are identified by the criteria adopted by Liu et al. (2001) and Ogawa et al. (2009). The criteria for selecting ion upflow are as follows: (1) Each profile is binned by height (every 50 km) and MLT of day (every 10 min). (2) Ion velocities for each height and time bins exceed 100 m/s at three or more consecutive heights (i.e., at the altitude range of at least 100 km) along the height profile. The resulting ion upflow events are displayed in the MLT and height coordinate in Figure 1a and height-integrated numbers of hourly events are presented in Figure 1b. We found that the ion upflow event mostly occurs in the above about 350-km altitude. The local time distributions of events show maximum at around the magnetic local noon but minimum at 1600–1900 MLT. The number of the event is mostly less than 100 per each 50-km height and 10-min MLT bin, which corresponds to about 10% of the whole profiles within the bin. More details will be discussed in the next sections. The relative occurrence frequency of ion upflow within each bin is defined by

$$F\ (h, \mathrm{MLT}) = \frac{n\ (h, \mathrm{MLT})}{N\ (h, \mathrm{MLT})} \times 100$$

where $n\ (h, \mathrm{MLT})$ is the number of profiles with ion upflow events in each bin and $N\ (h, \mathrm{MLT})$ is the total number of profiles in the bin. With regard to the ion upflow events in relation to ion and electron heatings, it is considered to be associated with them when they satisfy the following condition:

$$T_{i/e} - T^0_{i/e} \geq 200\ \mathrm{K}$$

The background temperatures for ions and electrons ($T^0_{i/e}$) are calculated from 2-hr running average of ion and electron temperatures for each bin. The temperature data points with ion upflow events are excluded from the calculation of the background temperature (Ogawa et al., 2009, 2010).

3. Results and Discussions

Before we present the results of the analysis, it needs to be mentioned whether the location of the ESR observation is in the auroral oval or in the polar cap region. Figure 2 shows the approximate locations of ESR relative to the auroral oval boundaries on the Northern Hemisphere. This figure is adopted from Xiong et al. (2014), which statically determined the auroral oval boundaries using 10-year CHAMP magnetic field data. The boundaries of the auroral oval vary with magnetic activity as expected but show no dependence on solar extreme ultraviolet flux or season. Note that the poleward boundary near the MLT midnight does not vary with *Kp* level. According to these variations of the auroral boundaries, we can conclude that the ESR during quiet period ($Kp < 2$) is largely located in the auroral oval except for around the MLT midnight where it is nearly always in the polar cap region regardless of the magnetic activity level. On the other hand, during disturbed periods ($Kp \geq 4$), the ESR is mostly located in the polar cap region except for around the MLT noon where it becomes closer to the poleward boundary within the auroral oval. The results of this study should be discussed with this information of the ESR location.

3.1. Occurrence of Ion Upflow in Association With Ion/Electron Heating

To examine the characteristics of the occurrence of ion upflow in association with ion and electron heatings, we classified the ion upflow events as follows: (1) Type 1 includes the ion upflow events with the increase of

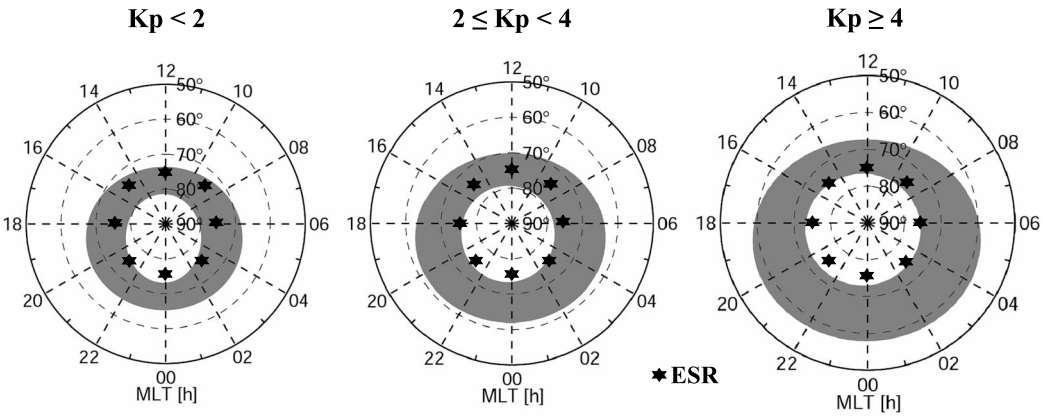

Figure 2. Approximate location of ESR in the varying auroral oval with different *Kp* levels adopted from Xiong et al. (2014). ESR = European Incoherent Scatter Svalbard Radar; MLT = magnetic local time.

ion temperature alone; (2) Type 2 includes the ion upflow events with the increase of electron temperature alone; (3) Type 3 includes the ion upflow events with the increase of both ion and electron temperatures; (4) Type 4 includes the ion upflow events without any increase of ion or electron temperature. Figure 3 shows the height versus MLT distributions of the relative occurrence frequency for four types. First of all, the occurrence of Type 2 with electron heating alone (up to 4%) is overall larger than those of Type 1 with ion heating alone (up to 1%), which indicates that the effect of electron heating is more effective to produce ion upflow than the heating of ion itself. However, the largest occurrence frequency occurs when both the ions and electrons are heated as in Type 3. Skjæveland et al. (2011) also found that the greatest upflow events occurred in the cusp region when both ion and electron temperatures were enhanced. This result may imply that the upward moving electrons are much more effective to pull the ions up to higher

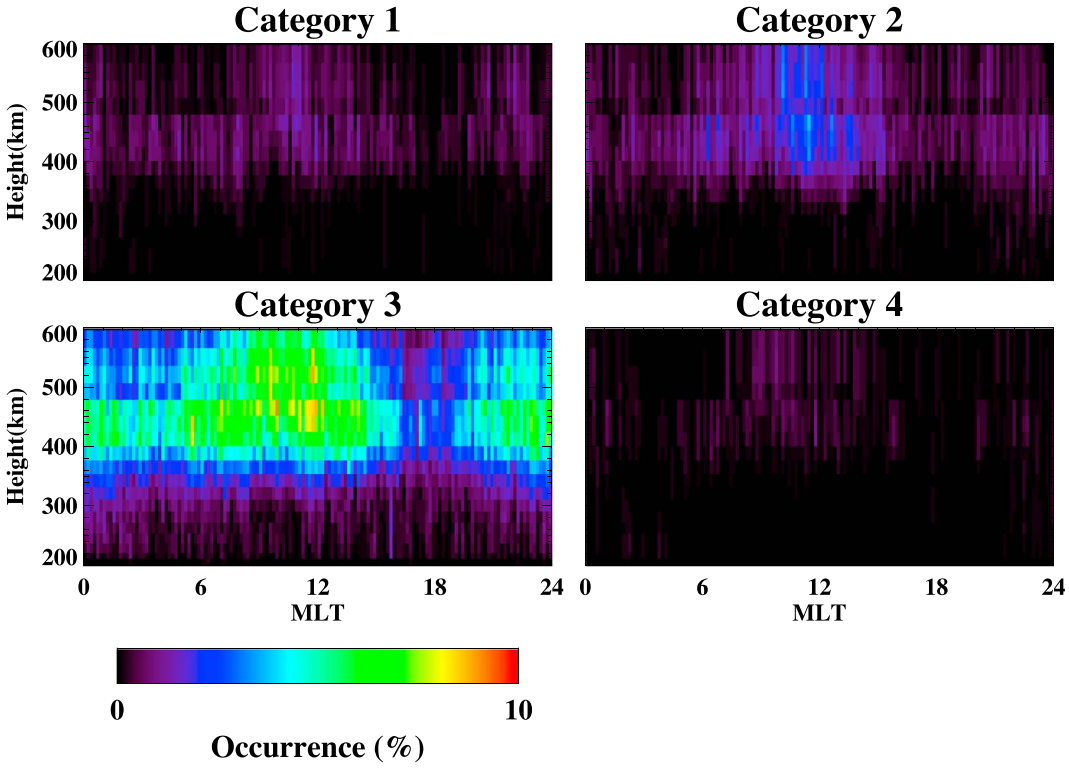

Figure 3. Height versus magnetic local time distributions of ion upflow occurrence for four Types as indicated in the figure: Type 1 with only ion heating, Type 2 with only electron heating, Type 3 with both ion and electron heatings, Type 4 without any heating.

altitude when the ions are also heated. Finally, when there are no electron and ion heatings (Type 4), our result shows that the occurrence frequency is negligibly small, which is different from Ogawa et al. (2009). They reported that approximately 40% of ion upflow events is not accompanied by any noticeable ion/electron heating from the analysis of the ESR data during the period of 1997 to 2006. However, they did not provide any discussion on this result. We do not know why the results are so different from each other, but there are some differences both in the observation period and analysis procedures. The observation period for this study is from 2000 to 2015, which is much longer than the period for Ogawa et al. (2009). We used data only from 42-m antenna of ESR, pointing in the field-aligned direction, but they used data from 32-m antenna as well as 42-m antenna. There may also be differences in the analysis procedures such as data binning and the criteria for identifying the ion upflow events.

3.2. Local Time Variations of the Occurrence of Ion Upflow

In Figures 1 and 3, it is found that the occurrence frequency is highest in the daytime between about 08:00 and 14:00 MLT but lowest at around the sunset. There exist appreciable ion upflow events even at night. It should be noted that the ion upflow occurrences are largely similar for all types in terms of local time and height distributions. The local time sector with the lowest occurrence at around the sunset spans from the late afternoon at around 15:00 MLT to the evening at about 20:00 MLT. This result was also found at Ogawa et al. (2009), which studied the characteristics of ion upflow in Svalbard (75.2° magnetic latitude) using the ESR data. Liu et al. (2001) described it as a dawn-dusk asymmetry using only 1-year ESR data. However, these characteristic local time variations in Svalbard do not appear in Tromso, mostly located in the auroral oval. Ogawa et al. (2010) analyzed field-aligned data obtained from the EISCAT Tromso ultra-high frequency radar during the period of 1984 to 2008 and found that the ion upflow most frequently occurs in the nighttime between 20:00 and 04:00 MLT but barely occurs during the daytime, which is almost opposite to the ion upflow occurrence in Svalbard. This result was also presented at Liu et al. (2001) by using the observations from ESR and EISCAT. The different characteristics of the occurrence in the two regions imply that two different physical processes exist in the regions to produce the ion upflow. The minimum occurrence of ion upflow at dusk appears only near the polar cap region, but not in the auroral oval, which needs to be further studied.

Regarding the daytime enhancement, as the ESR radar site approaches to the cusp region as the Earth rotates, the occurrence frequency of ion upflow substantially increases near the magnetic local noon since the soft particle precipitation is enhanced to heat electrons (Liu et al., 2001; Ogawa et al., 2009; Su et al., 1999). The dayside polar cap ionosphere near the cusp region is a highly dynamic region that shows transient plasma flows and shears due to large energy flux coming from the magnetosphere (Pitout et al., 2001; Skjæveland et al., 2011). In particular, the soft particle precipitation occurring in this region heats electrons at high altitudes, and therefore, it can more efficiently drive ions upward with them. The more energetic electrons penetrate deep into low altitudes where the upward motion of ions is less effective due to the collisions with dense neutrals. In this dynamically active region, the ion upflow can readily be caused by ion and electron heatings (Skjæveland et al., 2011).

The height distributions of the occurrence frequency are highest in the altitude range of about 350–500 km for most of local times, but it is extended up to 600-km height during the daytime. Around the magnetic local noon sector, there seem to be additional processes to cause the ion upflow in the altitude region above about 500 km, which may be associated with the soft particle precipitation described above. The vertical distributions of ion upflow will be further discussed in the next section.

3.3. Vertical Extent of the Ion Upflow Events

Figure 4 shows the number of ion upflow events with vertical extents in the altitude range of 200 to 1,000 km. It is assumed that each ion upflow event starts from their initial altitudes and stops upward motion at the final altitudes in each bin profile. For this analysis the top boundary altitude is extended to 1,000 km to investigate the vertical extent of the ion upflow events over 400-km height range even if the ISR data at the altitude above about 600 km is known to have low signal-to-noise ratios. The vertical extent of each ion upflow event indicates how far the ions can move up to higher altitudes once the upflow events are initiated at each initial altitude. In Figure 4, the mean vertical extents and corresponding numbers of events are presented for each initial altitude between 200 and 600 km with a 50-km step for Types 1 to 4. Note that the range of the

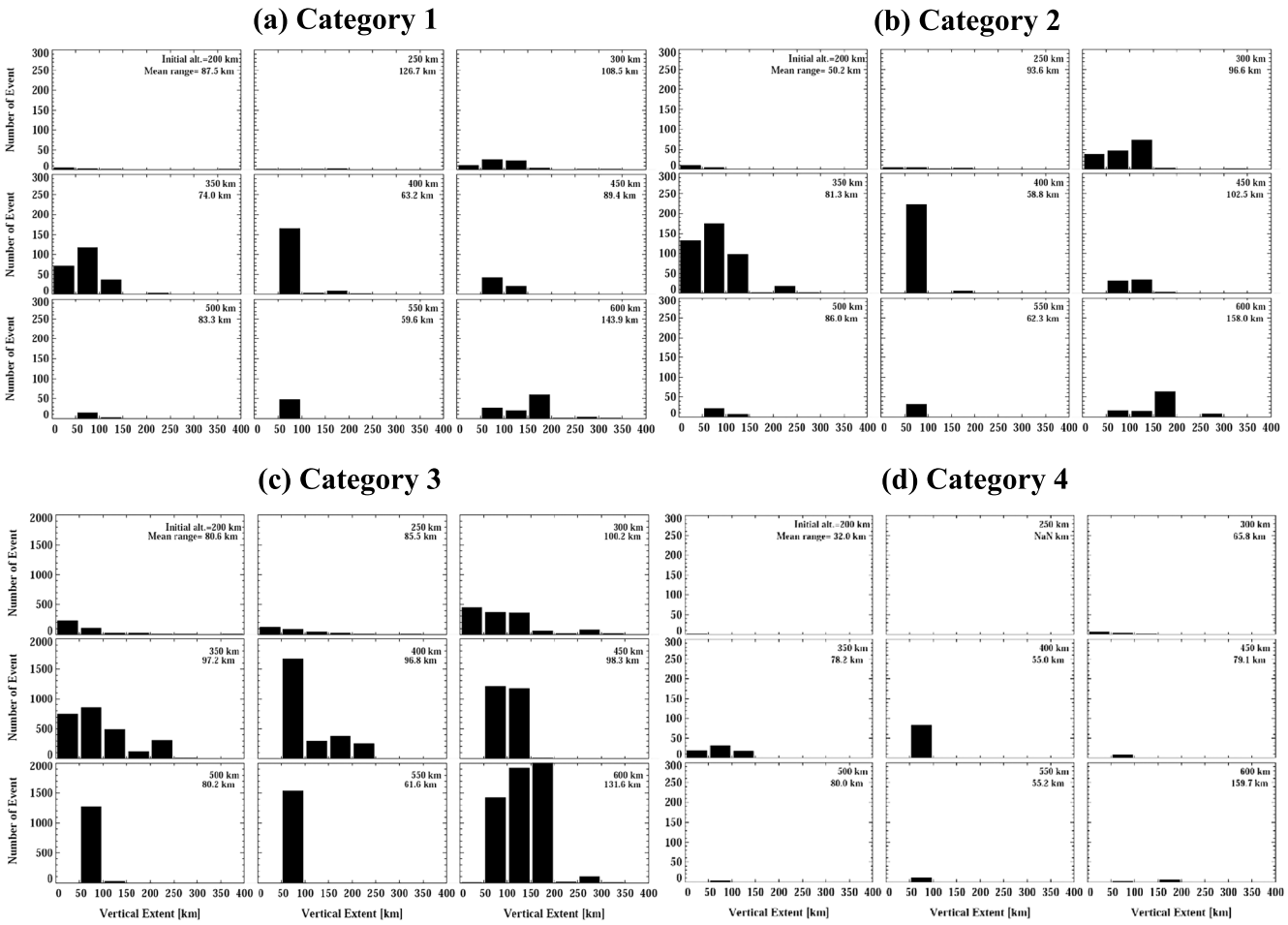

Figure 4. Vertical extents of ion upflow events initiated from 200- to 600-km altitude: (a) Type 1, (b) Type 2, (c) Type 3, and (d) Type 4.

number of events for Type 3 is much larger than the others: 0–2,000 versus 0–300, which indicates that the number of events for Type 3 is overwhelmingly larger than the other types, as already implied in Figure 3. The ion upflow events are hardly initiated below 300-km altitude for all types. There are appreciable amount of ion upflow events initiated even at 600-km altitude. The vertical extents of the ion upflows are mostly less than 200 km, which implies that the ion upflows initiated at 600-km altitude can reach up to about 800-km altitude. This result indicates that most of the upflowing ions initiated below about 600 km may not reach high enough to be further accelerated by wave activity to become ion outflows but instead return back to the lower atmosphere (Nilsson et al., 2008; Ogawa et al., 2009; Skjæveland et al., 2014). On the other hand, there is a large amount of ion upflows initiated at the altitude of 600 km with the vertical extent of up to 200 km in Type 3 in Figure 4. These upflowing ions may reach to the high altitude where the wave activity can transfer additional energy for the ions to be outflows. As seen in Figure 3, these ion upflows reaching high altitude mostly occur at around the magnetic local noon, in other words, near the ionospheric polar cusp region. Skjæveland et al. (2014) found that the upflowing plasma below 500-km altitude was unlikely to reach to about 800-km altitude, but the upflowing plasma above 600-km altitude was very likely to move to higher altitude and eventually become outflows when there are additional forces to further accelerate them. As mentioned earlier in this section, however, it should be kept in mind that the ISR data above 600-km altitude may have a limitation in the measurement accuracy due to low signal-to-noise ratios.

The MLT and height distributions of the relative occurrence frequency were similar for all four types as indicated in Figure 2. This is also true for different geomagnetic and solar activity conditions. Therefore, we

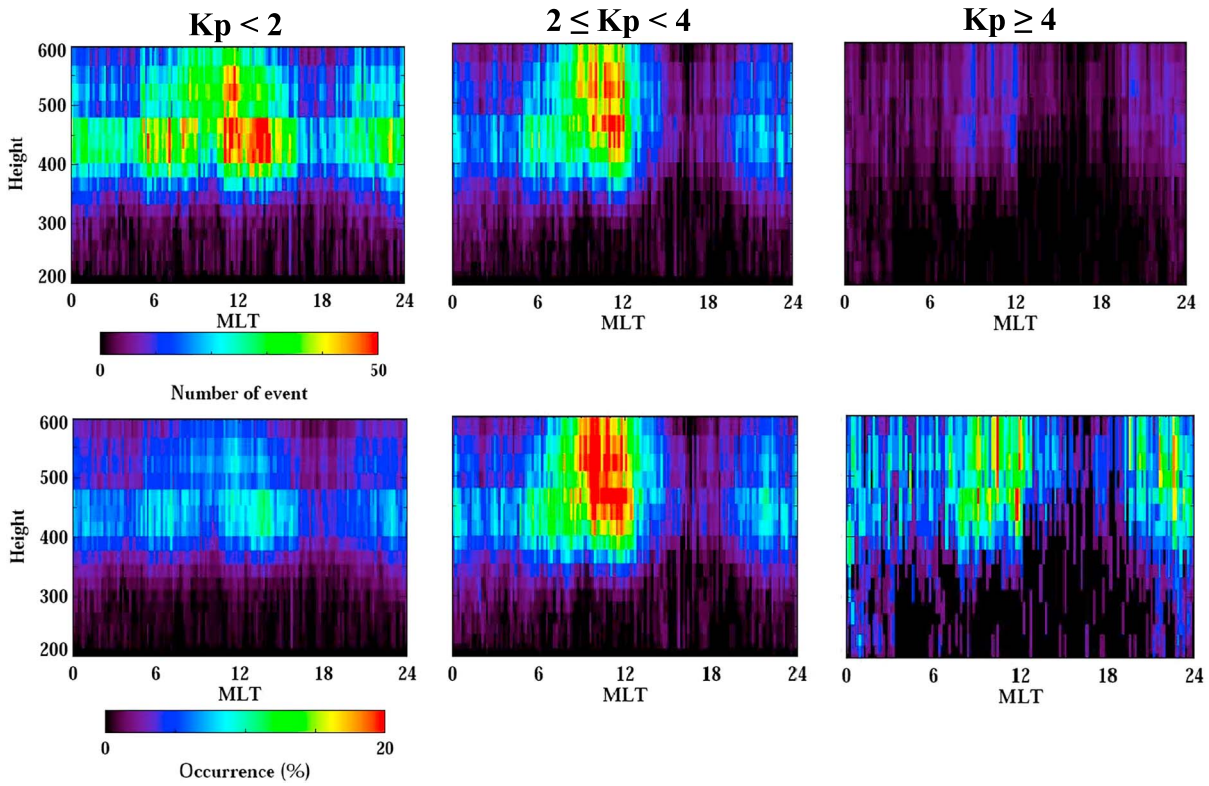

Figure 5. Height versus magnetic local time (MLT) distributions of the number of ion upflow events (top row) and ion upflow occurrence (bottom row) with three different *Kp* levels: low $Kp < 2$ (left column), medium $2 \leq Kp < 4$ (middle column), and high $Kp \geq 4$ (right column).

included all types of upflow events to investigate how the ion upflow occurrence varies with *Kp* and *F*10.7 indices as well as season in the following sections.

3.4. Occurrences of Ion Upflow With Geomagnetic Activity

The main physical mechanisms for the ion upflow are related to the electron and ion heatings induced by energetic particles and plasma convection, respectively. Therefore, they are in principle associated with the level of geomagnetic activity. The occurrence of ion upflow should be expected to show a close correlation with the *Kp* index. Figure 5 shows the height versus MLT distributions of the number of ion upflow events and the relative occurrence frequency with three different levels of *Kp* index. As *Kp* increases from low ($Kp < 2$) to medium ($2 \leq Kp < 4$), the local time distributions of the ion upflow show more significant diurnal variation with being much larger during the daytime than the nighttime and with a deeper and wider minimum near dusk. In other words, the ion upflow occurrence is significantly enhanced during the daytime, but little changed during the nighttime, which may provide some clue on the physical processes to cause the upflow. The deeper and wider minimum at dusk sector also indicates that the dusk minimum is relevant to geomagnetic activity, which requires a further investigation. Note that there seem to be two peaks in the daytime ion upflow for quiet times ($Kp < 2$), the first one in the morning sector (06:00–08:00 MLT) and the second and larger one at around the noon (12:00–14:00 MLT) but the double peak structure disappears and only one peak appears just before the magnetic noon (10:00–12:00 MLT) for disturbed times. The daytime double peak structure of the ion upflow was also reported at Ogawa et al. (2011).

For high $Kp > 4$, although the number of upflow events in the top panels of Figure 5 seems to negligibly be small, compared with smaller *Kp* conditions, the upflow occurrence in the bottom panels seems to show somewhat different characteristics of the distribution. First of all, the daytime occurrence is remarkably smaller than for medium *Kp* but the nighttime occurrence is still significant, particularly before midnight, and even in the lower altitude below 400 km at around midnight. However, the results for $Kp > 4$ may not necessarily be presenting the magnetic activity dependence of the ion upflow but it may only be related to the relative change of ESR location with geomagnetic activity as shown in Figure 2. The smaller

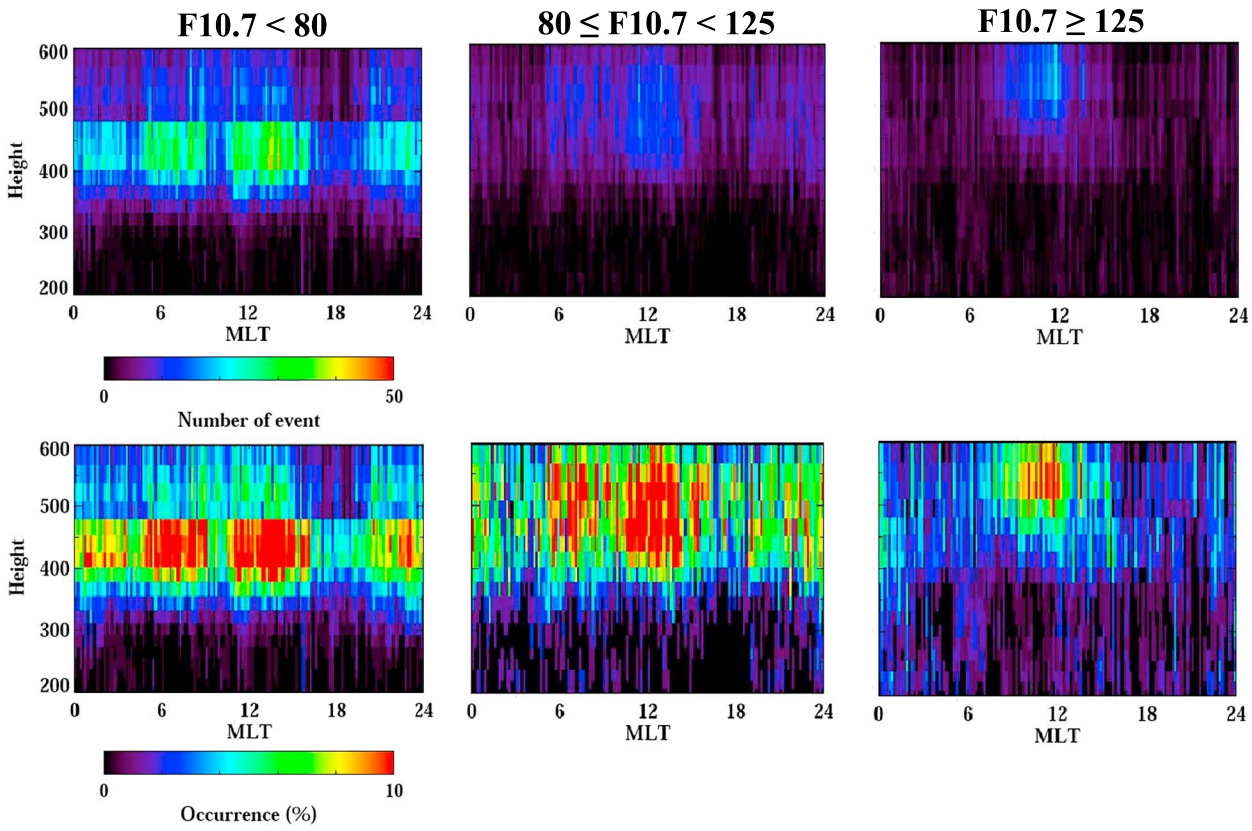

Figure 6. Height versus magnetic local time (MLT) distributions of the number of ion upflow events (top row) and ion upflow occurrence (bottom row) with three different $F10.7$ cm indices: $F10.7 < 80$ (left column), $80 \leq F10.7 < 125$ (middle column), and $F10.7 \geq 125$ (right column).

occurrence at around the noon for $Kp > 4$ may indicate that the ESR site is off the cusp region, which reduces the effects of soft electron precipitation. At around the midnight, the ESR site keeps staying in the polar cap region and then the enhanced frictional heating and more energetic electron precipitation with increased Kp may have affected to increase the upflow occurrence even in the lower altitude region. Ogawa et al. (2009) also reported that the probability of observing daytime ion upflow increases with Kp until $Kp \sim 3$ but decreases when $Kp > 3$, which largely agrees with our result for daytime ion upflow.

3.5. Occurrence of Ion Upflow With Solar Activity

While the geomagnetic activity affects the ion upflow by changing the energy inputs from the magnetosphere, the solar activity may affect it by changing the ionospheric and thermospheric states. Cohen et al. (2015) investigated the ion upflow dependence on the ionospheric density and solar photoionization from the model simulation of ion upflow driven by auroral precipitation. Their study showed that the increased ionospheric density reduces ion upflow occurrence due to smaller electron heating and resulting weaker ambipolar electric field. Figure 6 shows the height versus MLT distributions of the number of ion upflow events and the relative occurrence frequency with three different $F10.7$ indexes. For this results, we used the data only for $Kp < 2$ in order to eliminate the geomagnetic effects. We found that the overall number of events as well as the occurrence of the ion upflow are clearly decreasing with increasing solar activity as suggested from the model simulation (Cohen et al., 2015). Furthermore, the peak height of the ion upflow occurrence moves to higher altitude with increasing solar activity from 350- to 450-km altitude to about 450- to 550-km altitude for medium $F10.7$ and then to above about 500-km altitude for high $F10.7$.

As the solar activity increases, the upper atmosphere including the ionosphere and thermosphere is heated with enhanced photoionization and then the whole upper atmosphere is expanded upward, which results in the enhanced neutral density in the upper atmosphere as well as the increased ionospheric peak height. These changes in the ionosphere and neutral atmosphere require more energy to move the ions upward

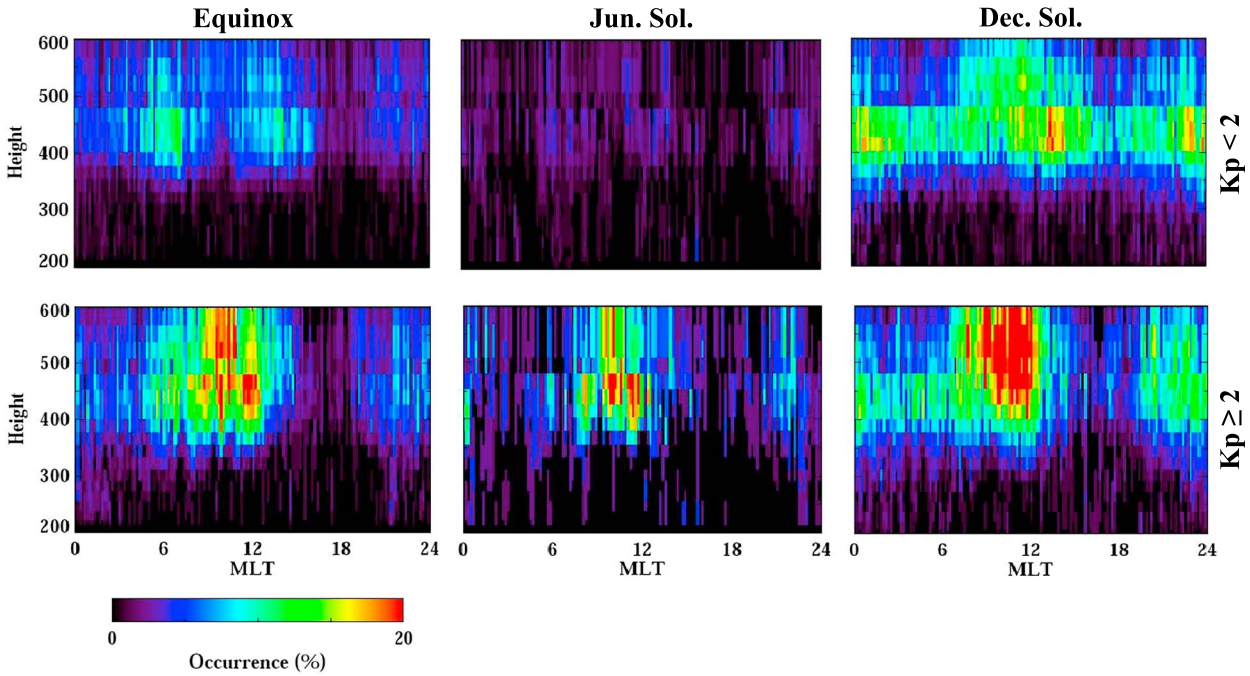

Figure 7. Height versus magnetic local time (MLT) distributions of ion upflow occurrence with three seasonal periods: equinox (left column), June solstice (middle column), and December solstice (right column). It is presented for quiet ($Kp < 2$) and moderately disturbed ($Kp \geq 2$) periods in the top and bottom panels, respectively.

(Ogawa et al., 2010), which explains decreased ion upflows with increasing solar activity. Under the given amount of energy for ion upflow, the enhanced ion density will decrease the average energy per ion and the enhanced neutral density will further reduce the ion upflow by increasing the friction between ions and neutrals. Regarding the increased peak height of the upflow occurrence, both the pressure gradient force of the ions and the ambipolar electric field are directed upward above the ionospheric density peak height. Therefore, the ion upflow tends to occur at higher altitude as the ionospheric peak height increases with increasing solar activity.

Note that while the peak height of the upflow increases with increasing solar activity, the ion upflow occurrence tends to increase at lower altitudes below the peak height. Ogawa et al. (2010) reported this low-altitude ion upflow for high solar activity, though not in the polar cap but in the auroral oval, and suggested that the vertical neutral motion may be responsible for it.

The double peak structure appeared for low *Kp* in Figure 5 becomes weak and eventually vanishes as solar activity increases in spite of the same low *Kp* condition. This result indicates that the double peak structure of the ion upflow appears only for geomagnetically quiet and low solar activity conditions. This characteristics of the daytime ion upflow occurrence with magnetic and solar activity conditions should be related to the physical processes responsible for causing ion upflow and requires further investigation.

3.6. Occurrence of Ion Upflow With Season

Figure 7 shows the height versus MLT distributions of the relative occurrence frequency for quiet ($Kp < 2$) and moderately disturbed ($Kp \geqq 2$) geomagnetic conditions during three seasonal periods as indicated in the figure. The seasonal bins are equinox (days of year: 50–110 and 234–294), June solstice (111–233), and December solstice (1–50 and 295–366). The occurrence of ion upflow shows overall maximum in December solstice and minimum in June solstice. The similar seasonal differences of the occurrence were also reported by Liu et al. (2001) and Buchert et al. (2004); the occurrence is higher in winter than in summer. This seasonal characteristics could be explained as in the previous section for solar activity dependence: The ion upflow tends to be more easily generated in winter than in summer, probably due to the smaller ion and neutral densities in winter.

The double peak structure for quiet times ($Kp < 2$) is present only in Equinox and June solstice but does not appear in December solstice, and as expected, it disappears for moderately disturbed condition even in equinox and June solstice.

4. Summary and Conclusion

Using 16-year EISCAT Svalbard radar (ESR) observations between 2000 and 2015, we investigated the statistical characteristics of ion upflow occurrence associated with ion and electron heatings. During quiet times, the ESR radar is mostly located in the auroral oval except for around the MLT midnight, but during disturbed times it is mostly located in the polar cap except for around the MLT noon (Figure 2). Keeping these changes in mind, the statistical characteristics of the ion upflow occurrence can be summarized as follows:

1. The occurrence of ion upflow is larger with electron heating (Type 2) than with ion heating (Type 1), but it is largest when there exist both ion and electron heatings (Type 3).
2. The maximum occurrence appears in the daytime, particularly near the magnetic local noon but a distinctive deep minimum occurs at around the sunset.
3. The highest occurrence appears in the altitude region of about 350–450 km for most of the local time, but it is distributed in the more extensive region of 350–600 km near the magnetic local noon.
4. The ions can move up to only about 200 km above their initiated heights, which may be mostly too low to become ion outflows.
5. The occurrence of ion upflow shows more significant diurnal variations for medium magnetic activity: that is, larger daytime peak, deeper, and wider dusk minimum, but largely unchanged at night. For highest magnetic activity, however, these trends are not persistent probably because of the change of the ESR radar location with *Kp* level.
6. The occurrence of ion upflow tends to decrease and distributed at higher altitude with increasing solar activity probably due to the enhanced and elevated upper atmosphere.
7. The maximum occurrence of ion upflow appears in December solstice, but the minimum occurs in June solstice for most of local times. The daytime double peak structure disappears in winter.

In summary, the various characteristics of the ion upflow occurrence are revealed with local time, height, magnetic activity, solar activity, and season in association with electron and ion heatings. Most of these results still require further investigations and will contribute to the understanding of the physical aspects of the ion upflow in the polar region.

Acknowledgments
This study was supported by the Grant PE19020 from the Korea Polar Research Institute. The ESR data were obtained from the EISCAT database at NIPR (http://pc115.seg20.nipr.ac.jp/www/eiscatdata/list.html) and the Madrigal database (http://www.eiscat.se/madrigal/).

Reference

Buchert, S. C., Ogawa, Y., Fujii, R., & van Eyken, A. P. (2004). Observations of diverging field-aligned ion flow with the ESR. *Annals of Geophysics*, *22*(3), 889–899. https://doi.org/10.5194/angeo-22-889-2004

Burchill, J. K., Knudsen, D. J., Clemmons, J. H., Oksavik, K., Pfaff, R. F., Steigies, C. T., et al. (2010). Thermal ion upflow in the cusp ionosphere and its dependence on soft electron energy flux. *Journal of Geophysical Research*, *115*, A05206. https://doi.org/10.1029/2009JA015006

Cohen, I. J., Lessard, M. R., Varney, R. H., Oksavik, K., Zettergren, M., & Lynch, K. A. (2015). Ion uplfow dependence on ionospheric density and solar photoionization. *Journal of Geophysical Research: Space Physics*, *120*, 10,039–10,052. https://doi.org/10.1002/2015JA021523

David, T. W., Wright, D. M., Milan, S. E., Cowley, S. W. H., Davies, J. A., & McCrea, I. (2018). A study of observations of ionospheric upwelling made by the EISCAT Svalbard radar during the International Polar Year Campaign of 2007. *Journal of Geophysical Research: Space Physics*. https://doi.org/10.1002/2017JA024802

Endo, M., Fujii, R., Ogawa, Y., Buchert, S. C., Nozawa, S., Watanabe, S., & Yoshida, N. (2000). Ion upflow and downflow at the topside ionosphere observed by the EISCAT VHF radar. *Annals of Geophysics*, *18*(2), 170–181. https://doi.org/10.1007/s00585-000-0170-3

Foster, C., Lester, M., & Davies, J. A. (1998). A statistical study of diurnal, seasonal and solar cycle variations of F region and topside auroral upflows observed by EISCAT between 1984 and 1996. *Annals of Geophysics*, *16*(10), 1144–1158. https://doi.org/10.1007/s00585-998-1144-0

Ganguli, G., Keskinen, M. J., Romero, H., Hellis, R., Moore, T., & Pollock, C. (1994). Coupling of microprocesses and macroprocesses due to velocity shear: An application to the low-altitude ionosphere. *Journal of Geophysical Research*, *99*(A5), 8873. https://doi.org/10.1029/93JA03181

Keating, J. G., Mulligan, F. J., Doyle, D. B., Winser, K. J., & Lockwood, M. (1990). A statistical study of large field-aligned flows of thermal ions at high latitudes. *Planetary and Space Science*, *9*, 1187.

Liu, C., Horwitz, J. L., & Richards, P. G. (1995). Effects of frictional heating and soft-electron precipitation on high-latitude F-region upflows. *Geophysical Research Letters*, *22*(20), 2713–2716. https://doi.org/10.1029/95GL02551

Liu, H., & Lu, G. (2004). Velocity shear-related ion upflow in the low-altitude ionosphere. *Annals of Geophysics*, *22*(4), 1149–1153. https://doi.org/10.5194/angeo-22-1149-2004

Liu, H., Ma, S.-Y., & Schlegel, K. (2001). Diurnal, seasonal and geomagnetic variations of large field-aligned ion upflows in the high-latitude ionospheric F region. *Journal of Geophysical Research*, *106*(A11), 24,651–24,661. https://doi.org/10.1029/2001JA900047

Loranc, M., Hanson, W. B., Heelis, R. A., & St, J.-P. (1991). Maurice, A morphological study of vertical ionospheric flows in the high-latitude F-region. *Journal of Geophysical Research*, *96*(A3), 3627. https://doi.org/10.1029/90JA02242

Ma, Y. Z., Zhang, Q.-H., Xing, Z.-Y., Jayachandran, P. T., Moen, J., Heelis, R. A., & Wang, Y. (2018). Combined contribution of solar illumination, solar activity, and convection to ion upflow above the polar cap. *Journal of Geophysical Research: Space Physics*, *123*, 4317–4328. https://doi.org/10.1029/2017JA024974

McCrea, I. W., Lockwood, M., Moen, J., Pitout, F., Eglitis, P., Aylward, A. D., et al. (2000). ESR and EISCAT observations of the response of the cusp and cleft to IMF orientation changes. *Annals of Geophysics*, *18*(9), 1009–1026. https://doi.org/10.1007/s00585-000-1009-7

Moen, J., Oksavik, K., & Carlson, H. C. (2004). On the relationship between ion upflow events and cusp auroral transients. *Geophysical Research Letters*, *31*, L11808. https://doi.org/10.1029/2004GL020129

Nilsson, H., Waara, M., Marghitu, O., Yamauchi, M., Lundin1, R., Reme, H., et al. (2008). Transients in oxygen outflow above the polar cap as observed by the Cluster spacecraft. *Annals of Geophysics*, *26*(11), 3365–3373. https://doi.org/10.5194/angeo-26-3365-2008

Ogawa, Y., Buchert, S. C., Fujii, R., Nozawa, S., & van Eyken, A. P. (2009). Characteristics of ion upflow and downflow observed with the European Incoherent Scatter Svalbard radar. *Journal of Geophysical Research*, *114*, A05305. https://doi.org/10.1029/2008JA013817

Ogawa, Y., Buchert, S. C., Häggström, I., Rietveld, M. T., Fujii, R., Nozawa, S., & Miyaoka, H. (2011). On the statistical relation between ion upflow and naturally enhanced ion-acoustic lines observed with the EISCAT Svalbard radar. *Journal of Geophysical Research*, *116*, A03313. https://doi.org/10.1029/2010JA015827

Ogawa, Y., Buchert, S. C., Sakurai, A., Nozawa, S., & Fujii, R. (2010). Solar activity dependence of ion upflow in the polar ionosphere observed with the European Incoherent Scatter (EISCAT) Tromsø UHF radar. *Journal of Geophysical Research*, *115*, A07310. https://doi.org/10.1029/2009JA014766

Ogawa, Y., Fujii, R., Buchert, S. C., Nozawa, S., & Ohtani, S. (2003). Simultaneous EISCAT Svalbard radar and DMSP observations of ion upflow in the dayside polar ionosphere. *Journal of Geophysical Research*, *108*(A3), 1101. https://doi.org/10.1029/2002JA009590

Pitout, F., Bosqued, J.-M., Alcaydé, D., Denig, W. F., & Réme, H. (2001). Observations of the cusp region under northward IMF. *Annals of Geophysics*, *19*(10/12), 1641–1653. https://doi.org/10.5194/angeo-19-1641-2001

Skjæveland, Å., Moen, J., & Carlson, H. C. (2014). Which cusp upflow events can possibly turn into outflows? *Journal of Geophysical Research: Space Physics*, *119*, 6876–6890. https://doi.org/10.1002/2013JA019495

Skjæveland, Å., Moen, J. I., & Carlson, H. C. (2011). On the relationship between flux transfer events, temperature enhancements and ion upflow events in the cusp ionosphere. *Journal of Geophysical Research*, *116*, A10305. https://doi.org/10.1029/2011JA016480

Su, Y.-J., Caton, R. G., Horwitz, J. L., & Richards, P. G. (1999). Systematic modeling of soft-electron precipitation effects on high-latitude *F* region and topside ionospheric upflows. *Journal of Geophysical Research*, *104*(A1), 153–163. https://doi.org/10.1029/1998JA900068

Winser, K. J., Jones, G. O. L., Williams, P. J. S., & Lockwood, M. (1989). Observations of large field-aligned flows of thermal plasma in the auroral ionosphere. *Advances in Space Research*, *9*(5), 57–63. https://doi.org/10.1016/0273-1177(89)90341-4

Wu, X.-Y., Horwitz, J. L., & Seo, Y. (2000). Statistical analysis of F region and topside ionospheric ion field-aligned flows at high latitudes. *Journal of Geophysical Research*, *105*(A2), 2477–2494. https://doi.org/10.1029/1999JA900437

Xiong, C., Lühr, H., Wang, H., & Johnsen, M. G. (2014). Determining the boundaries of the auroral oval from CHAMP field-aligned current signatures—Part 1. *Annals of Geophysics*, *32*(6), 609–622. https://doi.org/10.5194/angeo-32-609-2014

Zhang, Q.-H., Zong, Q. G., Lockwood, M., Heelis, R. A., Hairston, M., Liang, J., et al. (2016). Earth's ion upflow associated with polar cap patches: Global and in situ observations. *Geophysical Research Letters*, *43*, 1845–1853. https://doi.org/10.1002/2016GL067897

Zhao, K., Jiang, Y., Chen, K. W., & Huang, L. F. (2016). Geomagnetic and solar activity dependence of ionospheric upflowing O+: FAST observations. *Astrophysics and Space Science*, *361*(9). https://doi.org/10.1007/s10509-016-2872-3